Large-scale structure formation with global topological defects

Ruth Durrer* and Zhi-Hong Zhou
Universität Zürich, Institut für Theoretische Physik, Winterthurerstrasse 190, CH-8057 Zürich, Switzerland
(Received 18 July 1995)

We investigate cosmological structure formation seeded by topological defects which may form during a phase transition in the early Universe. First, we derive a partially new, local, and gauge-invariant system of perturbation equations to treat microwave background and dark matter fluctuations induced by topological defects or any other type of seeds. We then show that this system is well suited for numerical analysis of structure formation by applying it to seeds induced by fluctuations of a global scalar field. Our numerical results cover a larger dynamical range than those covered by previous investigations and are complementary to them since we use substantially different methods. The resulting microwave background fluctuations are compatible with older simulations. We also obtain a scale-invariant spectrum of fluctuations although with somewhat higher amplitude. On the other hand, our dark matter results yield a smaller bias parameter compatible with $b\sim 2$ on scales of $20h^{-1}$ Mpc in contrast with previous work which yielded larger bias factors. Our conclusions are thus more positive. According to the aspects analyzed in this work, global topological defect-induced fluctuations yield viable scenarios of structure formation and do better than standard CDM on large scales. [S0556-2821(96)00510-3]

PACS number(s): 98.80.Cq, 98.80.Bp, 98.80.Hw

I. INTRODUCTION

The formation of cosmological structure in the Universe, inhomogeneities in the matter distribution such as quasars at redshifts up to $z\sim 5$, galaxies, clusters, super clusters, voids, and walls, is an outstanding basically unsolved problem within the standard model of cosmology. At first sight, it seems obvious that small density enhancements can grow sufficiently rapidly by gravitational instability. But global expansion of the Universe and radiation pressure counteract gravity, so that, e.g., in the case of a radiation-dominated, expanding Universe, no density inhomogeneity can grow faster than logarithmically. Even in a Universe dominated by pressureless matter, cosmic dust, the growth of density perturbations is strongly reduced by the expansion of the Universe.

On the other hand, we know that the Universe was extremely homogeneous and isotropic at early times. This follows from the isotropy of the 3 K cosmic microwave background (CMB), which represents a relic of the plasma of baryons, electrons, and radiation at times before protons and electrons combined to form hydrogen. After a long series of upper bounds, measurements with the Cosmic Background Explorer (COBE) satellite have finally established anisotropies in this radiation [1] at the level of

$$\left\langle \frac{\Delta T}{T}(\theta)\right\rangle \sim 10^{-5} \text{ on angular scales } 7^\circ \leqslant \theta \leqslant 90^\circ.$$

On smaller angular scales, the observational situation is at present somewhat confusing and contradictory [2], but many upper limits require $\Delta T/T<4\times 10^{-5}$ on all scales $\theta<8^\circ$.

All observations together clearly rule out the simplest model of a purely baryonic universe with density parameter $\Omega\sim 0.1$ and adiabatic initial fluctuations (either the initial perturbations are too large to satisfy CMB limits, or they are too small to develop into the observed large scale structure).

The most conservative way out, where one just allows for nonadiabatic initial perturbations (minimal isocurvature model), also faces severe difficulties [3–6]. In other models, one assumes that initial fluctuations are created during an inflationary epoch, but that the matter content of the Universe is dominated by hot or cold dark matter or a mixture of both. Dark matter particles do not interact with photons other than gravitationally and thus induce perturbations in the CMB only via gravitation. In these models, inflation generically leads to $\Omega=1$, while the baryonic density parameter is only $\Omega_B h^2\sim 0.01$, compatible with nucleosynthesis constraints. With one component of dark matter, these models do not seem to agree with observations [4,7], however, if a suitable mixture of hot and cold dark matter is adopted, the results from numerical simulations look quite promising [8–10], although they might have difficulties to account for the existence of clusters at a redshift $z\sim 1$ [11].

In these dark matter models initial fluctuations are generated during an inflationary phase. Since all worked out models of inflation face difficulties (all of them have to invoke fine tuning to obtain the correct amplitude of density inhomogeneities), we consider it very important to investigate yet another possibility: Density perturbations in dark matter and baryons might have been triggered by seeds. Seeds are an inhomogeneously distributed form of energy which makes up only a small fraction of the total energy density of the Universe. Particularly, natural seeds are topological defects. They can form during symmetry-breaking phase transitions in the early Universe [12,13]. Depending on the symmetry being gauged or global, the corresponding defects are called local or global.

*Present address: Université de Genève, Département de Physique Théorique, 24 quai E. Ansermet, CH-1211 Genève, Switzerland.

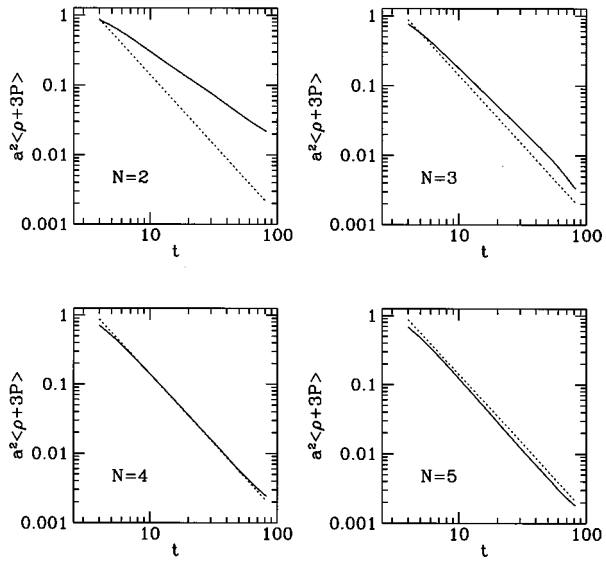

FIG. 1. The scaling behavior for $(\rho+3p)a^2$ found numerically in $(128)^3$ simulations for different O(N) models. The time is given in units of the grid spacing Δx. For comparison, a dashed line $\propto 1/t^2$ is also shown. After some initial oscillations, for $N>3$ the scaling is very clean until $t\sim 80$, where finite-size effects can become important.

The fluctuation spectrum on large scales observed by COBE is not very far from scale-invariant [14]. This has been considered a great success for inflationary models which generically predict a scale invariant fluctuation spectrum. However, as we shall see, also models in which perturbations are seeded by global topological defects, yield scale-invariant spectra of CMB fluctuations. To be specific, we shall mainly consider texture, π_3 defects which lead to event singularities in four-dimensional spacetime [15,16]. Global defects are viable candidates for structure formation, since the scalar field energy density ρ_S of global topological defects scales like $\rho_S \propto 1/(at)^2$ (up to a logarithmic correction for global strings) and thus always represents the same fraction of the total energy density of the Universe (t is conformal time):

$$\rho_S/\rho \sim 8\pi G\eta^2 \equiv 2\epsilon, \tag{1}$$

where η determines the symmetry-breaking scale (see Fig. 1). For the background spacetime we assume a Friedmann–Lemaître universe with $\Omega=1$ dominated by cold dark matter (CDM). We choose conformal coordinates such that

$$ds^2 = a^2(-dt^2+\delta_{ij}dx^i dx^j).$$

A numerical analysis of CMB fluctuations from topological defects on large scales has been performed in [17,18]; a spherically symmetric approximation is discussed in [19]. Results for intermediate scales angular are presented in [20]. All these investigations (except [19]) use linear cosmological perturbation theory in synchronous gauge and (except [18]) take into account only scalar perturbations. Here, we derive a fully gauge-invariant and local system of perturbation equations. The (nonlocal) split into scalar, vector, and tensor modes on hypersurfaces of constant time is not performed. We solve the equations numerically in a cold dark matter (CDM) universe with global texture. In this paper, we detail the results outlined in a previous letter [21]. Furthermore, we present explicit derivations of the equations, a description of our numerical methods, and we briefly discuss some tests of our codes. Since there is no spurious gauge mode in our initial conditions, there is no danger that these may grow in time and some of the difficulties to choose correct initial conditions (see, e.g., [18]) are removed. However, as we shall discuss in Sec. III, the results do depend very sensitively on the choice of initial conditions.

Nevertheless, we should keep in mind that we are investigating models of structure formation which rely on the particle physics and cosmology at temperatures of $T\sim T_{\rm GUT}\sim 10^{16}$ GeV. An energy scale about which we have no experimental evidence whatsoever. The physical model adopted for our calculations should thus always be considered as a toy model, which we hope, captures the features relevant for structure formation of the ''realistic physics'' at these energies. Therefore, we suggest, to not to take the results seriously much beyond about a factor of 2 or so. On the other hand, our models show that the particle physics at the grand unified theory (GUT) scale may have left its traces in the distribution of matter and radiation in the present Universe, yielding the exciting possibility to learn about the physics at the highest energies, smallest scales, by probing the largest structures of the Universe.

We calculate the CMB anisotropies on angular scales which are larger than the angle subtended by the horizon scale at decoupling of matter and radiation, $\theta>\theta_d$. For $\Omega=1$ and $z_d\approx 1000$,

$$\theta_d = 1/\sqrt{z_d+1} \approx 0.03 \approx 2^\circ. \tag{2}$$

It is therefore sufficient to study the generation and evolution of microwave background fluctuations after recombination. During this period, photons stream freely, influenced only by cosmic gravitational redshift and by perturbations in the gravitational field (if the medium is not reionized).

In Sec. II we derive a local and gauge-invariant perturbation equation to calculate the CMB fluctuations. In Sec. III, we put together the full system of equations which has to be solved to investigate gravitationally induced CMB fluctuations and the dark matter perturbation spectrum in a model with global topological defects. We discuss the choice of initial conditions and the numerical treatment of this system in Sec. IV. The next section is devoted to the presentation and analysis of our numerical results. We end with conclusions in Sec. VI.

Notation. We denote conformal time by t. Greek indices run from 0 to 3, Latin indices run from 1 to 3. The metric signature is chosen $(-+++)$. We set $\hbar=c=k_{\rm Boltzmann}=1$ throughout.

II. A LOCAL AND GAUGE-INVARIANT FORM OF THE PERTURBED LIOUVILLE EQUATION

Collisionless particles are described by their one-particle distribution function which lives on the seven-dimensional phase space:

$$\mathcal{P}_m = \{(x,p)\in T\mathcal{M} \,|\, g(x)(p,p) = -m^2\}.$$

Here, $\mathscr{M}$ denotes the spacetime manifold and $T\mathscr{M}$ its tangent space. The fact that collisionless particles move on geodesics translates to the Liouville equation for the one-particle distribution function f. The Liouville equation reads [22]

$$X_g(f)=0. \tag{3}$$

In a tetrad basis $(e_\mu)_{\mu=0}^3$ of $\mathscr{M}$, the vector field X_g on $\mathscr{P}_m$ is given by (see, e.g., [22])

$$X_g=\left(p^\mu e_\mu-\omega^i_\mu(p)p^\mu\frac{\partial}{\partial p^i}\right), \tag{4}$$

where ω^ν_μ are the connection one-forms of $(\mathscr{M},g)$ in the basis e^μ, and we have chosen the basis

$$(e_\mu)_{\mu=0}^3 \quad \text{and} \quad \left(\frac{\partial}{\partial p^i}\right)_{i=1}^3 \quad \text{on} \quad T\mathscr{P}_m, \quad p=p^\mu e_\mu .$$

We apply this general framework to the case of a perturbed Friedmann universe. The metric of a perturbed Friedmann universe with density parameter $\Omega=1$ is given by $ds^2=g_{\mu\nu}dx^\mu dx^\nu$ with

$$g_{\mu\nu}=a^2(\eta_{\mu\nu}+h_{\mu\nu})=a^2\tilde{g}_{\mu\nu}, \tag{5}$$

where $(\eta_{\mu\nu})=diag(-,+,+,+)$ is the flat Minkowski metric and $(h_{\mu\nu})$ is a small perturbation, $|h_{\mu\nu}|\ll 1$. We now use the fact that the motion of photons is conformally invariant.

We show that, for massless particles and conformally related metrics,

$$g_{\mu\nu}=a^2\tilde{g}_{\mu\nu},$$

$$(X_g f)(x,p)=0 \ \text{ is equivalent to } (X_{\tilde{g}}f)(x,ap)=0. \tag{6}$$

This is easily seen if we write X_g in a coordinate basis:

$$X_g=b^\mu\partial_\mu-\Gamma^i_{\alpha\beta}b^\alpha b^\beta\frac{\partial}{\partial b^i},$$

with

$$\Gamma^i_{\alpha\beta}=\frac{1}{2}g^{i\mu}(g_{\alpha\mu,\beta}+g_{\beta\mu,\alpha}-g_{\alpha\beta,\mu}).$$

The b^μ are the components of the momentum p with respect to the *coordinate* basis:

$$p=p^\mu e_\mu=b^\mu\partial_\mu .$$

If (e_μ) is a tetrad with respect to g, then $\tilde{e}_\mu=ae_\mu$ is a tetrad basis for $\tilde{g}$. Therefore, the coordinates of $ap=ap^\mu\tilde{e}_\mu=a^2p^\mu e_\mu=a^2b^\mu\partial_\mu$ with respect to ∂_μ on $(\mathscr{M},\tilde{g})$ are given by a^2b^μ. In the coordinate basis, thus our statement Eq. (6) follows, if we can show that

$$(X_{\tilde{g}}f)(x^\mu,a^2b^i)=0 \ \text{ if } (X_g f)(x^\mu,b^i)=0. \tag{7}$$

Setting $v=ap=v^\mu\tilde{e}_\mu=w^\mu\partial_\mu$, we have $v^\mu=ap^\mu$ and $w^\mu=a^2b^\mu$. Using $p^2=0$, we obtain the following relation for the Christoffel symbols of g and $\tilde{g}$:

$$\Gamma^i_{\alpha\beta}b^\alpha b^\beta=\tilde{\Gamma}^i_{\alpha\beta}b^\alpha b^\beta+\frac{2a_{,\alpha}}{a}b^\alpha b^i.$$

For this step it is crucial that the particles are massless. For massive particles, the statement is of course not true. Inserting this result into the Liouville equation, we find

$$a^2X_g f=w^\mu\left(\partial_\mu f|_b-2\frac{a_{,\mu}}{a}b^i\frac{\partial f}{\partial b^i}\right)-\tilde{\Gamma}^i_{\alpha\beta}w^\alpha w^\beta\frac{\partial f}{\partial w^i}, \tag{8}$$

where $\partial_\mu f|_b$ denotes the derivative of f with respect to x^μ at constant (b^i). Using

$$\partial_\mu f|_b=\partial_\mu f|_w+2\frac{a_{,\mu}}{a}b^i\frac{\partial f}{\partial b^i},$$

we see that the braces in Eq. (8) just correspond to $\partial_\mu f|_w$. Therefore,

$$a^2X_g f(x,p)=w^\mu\partial_\mu f|_w-\tilde{\Gamma}^i_{\alpha\beta}w^\alpha w^\beta\frac{\partial f}{\partial w^i}=X_{\tilde{g}}f(x,ap).$$

We have thus shown that the Liouville equation in a perturbed Friedmann universe is equivalent to the Liouville equation in perturbed Minkowski space,

$$(X_{\tilde{g}}f)(x,v)=0, \tag{9}$$

with[1]

$$v=v^\mu\tilde{e}_\mu=ap^\mu\tilde{e}_\mu .$$

We now want to derive a perturbation equation for Eq. (9). If $\overline{e^\mu}$ is a tetrad in Minkowski space, $\tilde{e}_\mu=\overline{e_\mu}+\frac{1}{2}h^\nu_\mu\overline{e_\nu}$ is a tetrad with respect to the perturbed geometry $\tilde{g}$. For $(x,v^\mu\overline{e_\mu})\in P_0$, thus, $(x,v^\mu\tilde{e}_\mu)\in\tilde{P}_0$. Here, P_0 denotes the zero-mass one-particle phase space in Minkowski space and $\tilde{P}_0$ is the phase space with respect to $\tilde{g}$, perturbed Minkowski space. We define the perturbation of the distribution function F by

$$f(x,v^\mu\tilde{e}_\mu)=\overline{f(x,v^\mu\overline{e_\mu})}+F(x,v^\mu\overline{e_\mu}). \tag{10}$$

Liouville's equation for f then leads to a perturbation equation for F. We choose the natural tetrad

$$\tilde{e}_\mu=\partial_\mu-\frac{1}{2}h^\nu_\mu\partial_\nu$$

with the corresponding basis of one-forms

$$\tilde{\theta}^\mu=dx^\mu+\frac{1}{2}h^\mu_\nu dx^\nu.$$

---

[1]Note that also Friedmann universes with nonvanishing spatial curvature, $K\neq 0$, are conformally flat and thus this procedure can also be applied for $K\neq 0$. Of course, in that case the conformal factor a^2 is no longer just the scale factor but depends on position. A coordinate transformation which transforms the metric of $K\neq 0$ Friedmann universes into a conformally flat form can be found, e.g., in [23].

Inserting this into the first structure equation, $d\tilde{\theta}^{\mu}=-\omega^{\mu}_{\nu}\wedge dx^{\nu}$, one finds

$$\omega_{\mu\nu}=-\frac{1}{2}(h_{\mu\lambda},_{\nu}-h_{\nu\lambda},_{\mu})\theta^{\lambda}.$$

Using the background Liouville equation, namely, that $\overline{f}$ is only a function of $v=ap$, we obtain the perturbation equation

$$(\partial_t+\gamma^i\partial_i)F=-\frac{v}{2}[(\dot{h}_{i0}-h_{00},_i)\gamma^i+(\dot{h}_{ij}-h_{0j},_i)\gamma^i\gamma^j]\frac{d\overline{f}}{dv},$$

where we have set $v^i=v\gamma^i$, with $v^2=\Sigma_{i=1}^{3}(v^i)^2$. Let us parametrize the perturbations of the metric by

$$(h_{\mu\nu})=\begin{pmatrix}-2A & B_i\\ B_i & 2H_L\delta_{ij}+2H_{ij}\end{pmatrix}, \tag{11}$$

with $H^i_i=0$. Inserting this above, we obtain

$$(\partial_t+\gamma^i\partial_i)F=-[\dot{H}_L+(A,_i+\tfrac{1}{2}\dot{B}_i)\gamma^i+(\dot{H}_{ij}-\tfrac{1}{2}B_{i,j})\gamma^i\gamma^j]v\frac{d\overline{f}}{dv}. \tag{12}$$

From Eq. (12) we see that the perturbation in the distribution function in each spectral band is proportional to $v\,d\overline{f}/dv$. This shows once more that gravity is achromatic. We thus do not lose any information if we integrate this equation over photon energies. We define

$$m=\frac{\pi}{\rho_r a^4}\int Fv^3dv.$$

$4m$ is the fractional perturbation of the brightness ι,

$$\iota=a^{-4}\int fv^3dv.$$

This is obtained using the relation

$$4\pi\int\frac{d\overline{f}}{dv}v^4dv=-4\int\overline{fv}^3dv\,d\Omega=-4\rho_r a^4. \tag{13}$$

Setting $\iota=\overline{\iota(T(\gamma,x))}$, one finds that $\iota=(\pi/60)T^4(\gamma,x)$. Hence, m corresponds to the fractional perturbation in the temperature:

$$T(\gamma,x)=\overline{T}(1+m(\gamma,x)). \tag{14}$$

Another derivation of Eq. (14) is given in [25]. Since the v dependence of F is of the form $v\,d\overline{f}/dv$, we have, with Eq. (13),

$$F(x^{\mu},\gamma^i,v)=-m(x^{\mu},\gamma^i)v\frac{d\overline{f}}{dv}.$$

This shows that m is indeed the quantity which is measured in a CMB anisotropy experiment, where the spectral information is used to verify that the spectrum of perturbations is the derivative of a blackbody spectrum. Of course, in a real experiment located at a fixed position in the Universe, the monopole and dipole contributions to m cannot be measured. They cannot be distinguished from a background component and from a dipole because of our peculiar motion with respect to the CMB radiation.

Multiplying Eq. (12) with v^3 and integrating over v, we obtain the equation of motion for m:

$$\partial_t m+\gamma^i\partial_i m=\dot{H}_L+(A,_i+\tfrac{1}{2}\dot{B}_i)\gamma^i+(\dot{H}_{ij}-\tfrac{1}{2}B_i,_j)\gamma^i\gamma^j. \tag{15}$$

It is well known that the equation of motion for photons only couples to the Weyl part of the curvature (null geodesics are conformally invariant). The right-hand side (RHS) of Eq. (15) is given by first derivatives of the metric only which could at most represent integrals of the Weyl tensor. To obtain a local, nonintegral equation, we thus rewrite Eq. (15) in terms of $\nabla^2 m$. It turns out that the most suitable variable is, however, not $\nabla^2 m$ but χ, which is given by

$$\chi=\nabla^2 m-(\nabla^2 H_L-\tfrac{1}{2}H,^{ij}_{ij})-\frac{1}{2}(\nabla^2 B_i-3\partial^j\sigma_{ij})\gamma^i,$$

where

$$\sigma_{ij}=-\frac{1}{2}(B_i,_j+B_j,_i)+\frac{1}{3}\delta_{ij}B^l_l+\dot{H}_{ij}.$$

Note that χ and $\nabla^2 m$ only differ by the monopole contribution, $\nabla^2 H_L-(1/2)H^{ij},_{ij}$ and the dipole contribution, $(1/2)\times(\nabla^2 B_i-3\partial^j\sigma_{ij})\gamma^i$. The higher multipoles of χ and $\nabla^2 m$ agree. An observer at fixed position and time cannot distinguish a monopole contribution from an isotropic background and a dipole contribution from a peculiar motion. Only the higher multipoles, $l\geqslant 2$, contain information about temperature anisotropies. For a fixed observer, therefore, we can identify $\nabla^{-2}\chi$ with $\delta T/T$.

In terms of metric perturbations, the electric and magnetic parts of the Weyl tensor are given by (see, e.g., [26,25])

$$E_{ij}=\frac{1}{2}[\triangle_{ij}(A-H_L)-\dot{\sigma}_{ij}-\nabla^2 H_{ij}-\tfrac{2}{3}H^{lm}_{lm}\delta_{ij}+H^l_{il},_j+H^l_{jl},_i], \tag{16}$$

$$B_{ij}=-\frac{1}{2}(\epsilon_{ilm}\sigma_{jm},_l+\epsilon_{jlm}\sigma_{im},_l), \tag{17}$$

with

$$\triangle_{ij}=\partial_i\partial_j-(1/3)\delta_{ij}\nabla^2.$$

Explicitly working out $(\partial_t+\gamma^i\partial_i)\chi$ using Eq. (15), yields after some algebra, the equation of motion for χ:

$$(\partial_t+\gamma^i\partial_i)\chi=3\gamma^i\partial^j E_{ij}+\gamma^k\gamma^j\epsilon_{kli}\partial_l B_{ij}\equiv S_T(t,\mathbf{x},\gamma), \tag{18}$$

where ϵ_{kli} is the totally antisymmetric tensor in three dimensions with $\epsilon_{123}=1$. The spatial indices in this equation are raised and lowered with δ_{ij} and thus index positions are irrelevant. Double indices are summed over irrespective of their positions.

Equation (18) is the main result of this section. We now discuss it, rewrite it in integral form, and specify initial conditions for adiabatic CDM perturbations plus seeds.

In Eq. (18) the contribution from the electric part of the Weyl tensor does not contain tensor perturbations. On the other hand, scalar perturbations do not induce a magnetic gravitational field. The second contribution to the source term in Eq. (18) thus represents a combination of vector and tensor perturbations. If vector perturbations are negligible, the two terms on the right-hand side (RHS) of Eq. (18) thus yield a split into scalar and tensor perturbations which is local.

Since the Weyl tensor of Friedmann Lemaître universes vanishes, the RHS of Eq. (18) is manifestly gauge invariant (this is the so-called Stewart-Walker lemma [28]). Hence, also the variable χ is gauge invariant. Another proof of the gauge invariance of χ, discussing the behavior of F under infinitesimal coordinate transformations, is presented in [25].

The general solution to Eq. (18) is given by

$$\chi(t,\boldsymbol{x},\gamma)=\int_{t_i}^{t} S_T(t',\boldsymbol{x}+(t'-t)\,\gamma,\gamma)dt' + \chi(t_i,\boldsymbol{x}+(t_i-t)\,\gamma,\gamma), \tag{19}$$

where S_T is the source term on the RHS of Eq. (18). Let us compare this result with the more familiar one, where one calculates $\delta T/T$ by integrating photon geodesics (which is of course equivalent to solving the Liouville equation). For simplicity, we specialize to the case of pure scalar perturbations [the expressions for vector and tensor perturbations given in [25] can be compared with Eq. (19) in the same manner]. For scalar perturbations, integration of photon geodesics yields [25]

$$\frac{\delta T}{T}(t_f,\boldsymbol{x}_f,\boldsymbol{n})=-\left[\tfrac{1}{4}D_g^{(r)}+V_i\cdot n^i+(\Psi-\Phi)\right]\Big|_i^f + \int_i^f(\dot\Psi-\dot\Phi)d\lambda. \tag{20}$$

Here, Ψ and Φ denote the Bardeen potentials as defined, e.g., in [27,25]. On super-horizon scales (which are the important scales for the Sachs-Wolfe contribution) $V_i\cdot n^i$ can be neglected. Furthermore, the contributions of the square brackets of Eq. (20) from the final time $t=t_f$, only lead to uninteresting monopole and dipole terms. We now use that the electric contribution to the Weyl tensor for purely scalar perturbations is given by [25]

$$E_{ij}=\frac{1}{2}(\partial_i\partial_j-\tfrac{1}{3}\delta_{ij}\nabla^2)(\Psi-\Phi)\equiv\frac{1}{2}\triangle_{ij}(\Psi-\Phi).$$

Therefore, $\partial_i(\Psi-\Phi)=3\partial^j E_{ij}$. Using furthermore

$$-(\Psi-\Phi)\Big|_i^f=-\int_i^f[\dot\Psi-\dot\Phi+(\Psi-\Phi)_{,i}n^i]d\lambda,$$

Eq. (20) leads to

$$\frac{\delta T}{T}(t,\boldsymbol{x},\boldsymbol{n})=\frac{1}{4}D_g^{(r)}(t_i,\boldsymbol{x}_i)-3\int_i^f\nabla^{-2}\partial^j E_{ij}n^i dt. \tag{21}$$

If we take into account that the direction $\boldsymbol{n}$ in Eq. (20), the direction of an *incoming* photon, corresponds to $-\gamma$ in Eq. (19), we find that Eq. (20) coincides with Eq. (19) for scalar perturbations, and that

$$\chi(t_i,\boldsymbol{x}_i,\gamma)=\frac{1}{4}\nabla^2 D_g^{(r)}(t_i,\boldsymbol{x}_i)=\frac{1}{4}\nabla^2 D_g^{(r)}(t_i,\boldsymbol{x}-(t-t_i)). \tag{22}$$

We now want to investigate this initial value and decompose Eq. (21) into terms caused by CDM and terms coming from the seeds, the scalar field. We assume that dark matter and radiation perturbations are adiabatic on *superhorizon scales*:

$$D_g^{(r)}=(4/3)D_g^{(c)}.$$

Since radiation and CDM probably have been a single fluid at very early times (e.g., at the time of the phase transition), this assumption is reasonable. It is, however, inconsistent to set $D_g^{(r)}=4/3D_g^{(c)}$ on subhorizon scales. Because of the different equations of state for the two components, adiabaticity cannot be maintained on subhorizon scales [27]. We can then derive, from Eqs. (2.36), (2.37), (2.45)–(2.47) in [25],

$$\frac{1}{4}D_g^{(r)}=\frac{5}{3}\Phi_C+\frac{2}{3}\dot\Phi_C/(\dot a/a)+\Phi_S$$

on superhorizon scales. Here, the Bardeen potentials are split into parts due to cold dark matter ($_C$) and the scalar field ($_S$), respectively. For cold dark matter, $\Psi_C=-\Phi_C$. Using this, we can bring Eq. (19) into the form

$$\frac{\delta T}{T}(t_f,\boldsymbol{x}_f,\boldsymbol{n})=\frac{1}{3}\Psi_C(t_i,\boldsymbol{x}_i)-\frac{2}{3}\dot\Psi_C/(\dot a/a)(t_i,\boldsymbol{x}_i) +2\int_i^f\dot\Psi_C dt+\Phi_S(t_i,\boldsymbol{x}_i) -\int_i^f\nabla^{-2}S_{TS}(t,\boldsymbol{x}_f-(t_f-t)\boldsymbol{n},\boldsymbol{n})dt, \tag{23}$$

where S_{TS} denotes the portion of the source term due to the scalar field only:

$$S_{TS}=-3n^i\partial^j E_{ij}^{(S)}+n^k n^j\epsilon_{klj}\partial_l B_{ij}^{(S)}. \tag{24}$$

From an analysis analogous to the one presented here for scalar perturbations, one can conclude that initial contributions to $\delta T/T$ from vector perturbations can be neglected on superhorizon scales and that those for tensor perturbations vanish. Equation (23) is thus the general solution on superhorizon scales, $\lambda\gg t_i$ for our adiabatic model (including vector and tensor perturbations of the seeds). Equation (23) is much better suited for numerical investigation than the general expression Eq. (19). This can be demonstrated by considering the case of pure CDM without source term: In this case, $\Phi_C=-\Psi_C=\text{const}$ and from Eq. (23) we easily recover the well-known result

$$\frac{\delta T}{T}(t,\boldsymbol{x},\boldsymbol{n})=\frac{1}{3}\Psi_C(t_i,\boldsymbol{x}-\boldsymbol{n}(t-t_i)),$$

whereas Eq. (19) in this case leads to

$$\frac{\delta T}{T}(t,\boldsymbol{x},\boldsymbol{n})=\frac{\delta T}{T}(t_i,\boldsymbol{x}_i,\boldsymbol{n})+2\Psi_C(t_i,\boldsymbol{x}_i).$$

In other words, the unknown initial condition in Eq. (19) cancels 5/6 of the naive result for the case of adiabatic CDM fluctuations. Even though because of the existence of $\dot{\Psi}_C$ terms, the cancellation is slightly less substantial in our case, the assumption of adiabaticity on superhorizon scales is a crucial ingredient of the model.

The electric and magnetic parts of the Weyl tensor are determined by the perturbations in the energy momentum tensor via Einstein's equations. We assume that the source for the geometric perturbations is given by the scalar field and dark matter. The contributions from radiation may be neglected. Furthermore, vector perturbations of dark matter (which decay quickly) are neglected. The divergence of E_{ij} is then given by (see the Appendix)

$$3\partial^j E_{ij}=8\pi G\rho_C a^2 D_i + 8\pi G\left[\partial_i\delta T_{00}+3\left(\frac{\dot{a}}{a}\right)\delta T_{0i}-(3/2)\partial^j\tau_{ij}\right], \tag{25}$$

where the first term on the RHS is the dark matter source term ρ_C, denoting the dark matter energy density. The second contribution is due to the scalar field: The energy momentum tensor of the scalar field

$$T^S_{\mu\nu}=\phi_{,\mu}\phi_{,\nu}-\frac{1}{2}g_{\mu\nu}\phi^{,\lambda}\phi_{,\lambda}$$

yields

$$\tau_{ij}\equiv T_{ij}-(a^2/3)\delta_{ij}T^l_l=\tau^S_{ij}=\phi_{,i}\phi_{,j}-(1/3)\delta_{ij}(\nabla\phi)^2,$$

$$\delta T_{0j}=T^S_{0j}=\dot{\phi}\phi_{,j},$$

$$\delta T_{00}=T^S_{00}=\frac{1}{2}[(\dot{\phi})^2+(\nabla\phi)^2],$$

and D_j is a gauge invariant perturbation variable for the density gradient. For scalar perturbations, $D_j=\partial_j D$. The evolution equation for the dark matter density perturbation is given by (see [24] and [29])

$$\ddot{D}_i+\left(\frac{\dot{a}}{a}\right)\dot{D}_i-4\pi G a^2\rho_C D_i=8\pi G\partial_i(\dot{\phi}^2). \tag{26}$$

During the radiation-dominated era $8\pi G\rho_R D_R$, in principle, has to be included in Eq. (26). But since radiation perturbations cannot grow substantially on subhorizon scales, and since dark matter fluctuations do not grow in a radiation-dominated universe [30], their influence is not very important. It leads to a slight decrease of the CDM perturbations. (We haved checked this and found differences of up to 20% on small scales but much less on large scales.)

The equation of motion for B_{ij} is more involved. A somewhat cumbersome derivation (see the Appendix) yields

$$a^{-1}(aB_{ij})^{\cdot\cdot}-\nabla^2 B_{ij}=8\pi G\mathscr{S}^{(B)}_{ij}, \tag{27}$$

with

$$\mathscr{S}^{(B)}_{ij}=-\epsilon_{lm(i}\delta T_{0l,j)m}+\epsilon_{lm(i}\dot{\tau}_{j)l,m}.$$

Here, $(i,\ldots,j)$ denote symmetrizations in indices i and j.

To the source term $\mathscr{S}^{(B)}$, only vector and tensor perturbations contribute. It is thus entirely determined by the energy momentum tensor of the scalar field.

Equations (23), (25), (26), and (27) constitute a fully local and gauge-invariant system of cosmological perturbation equations for CDM and photons in the presence of seeds.

III. THE SYSTEM OF EQUATIONS FOR GLOBAL SCALAR FIELD-INDUCED FLUCTUATIONS

In this section we collect all the equations which determine the system under consideration. We also repeat equations which have been derived in Sec. II. Let us begin with the scalar field equation of motion.

The energy momentum tensor of the scalar field is a small perturbation. In first-order perturbation theory, we can thus solve the equation of motion of the scalar field in the background, Friedmann-Lemaître geometry, neglecting geometric perturbations. The equation of motion for the scalar field ϕ is given by

$$g^{\mu\nu}\nabla_\mu\nabla_\nu\phi+\frac{\partial V}{\partial\phi}=0, \tag{28}$$

where $g^{\mu\nu}$ denotes the unperturbed metric and ∇_μ is the covariant derivative with respect to this metric. For our numerical computations, we consider an $O(4)$ model. In O(N) models, the scalar field $\phi\in\boldsymbol{R}^N$ and the zero-temperature potential is given by $V_0=\lambda/4(\phi^2-\eta^2)^2$ for some energy scale η. At high temperatures, $T>T_c\sim\eta$, one-loop corrections to the effective potential dominate and the minimum of the effective potential is at $\phi=0$. Below the critical temperature, the minimum is shifted (in the simplest case) to $\langle\phi^2\rangle=[1-(T/T_c)^2]\eta^2$ (see [12,16] and references therein). The vacuum manifold, i.e., the space of minima of the effective potential, then becomes a $(N-1)$-sphere, $\boldsymbol{S}^{(N-1)}$. Since

$$\pi_k(\boldsymbol{S}^m)=\begin{cases}0, & k<m,\\ \boldsymbol{Z}, & k=m,\end{cases}$$

the lowest nonvanishing homotopy group of a m-sphere is always π_m. Since probably higher defects are unstable and decay into lower ones,[2] the m-sphere is a suitable vacuum manifold to study π_m defects.

If the system under consideration is at a temperature T much below the critical temperature, $T\ll T_c$, it becomes more and more improbable for the field ϕ to leave the vacuum manifold. ϕ will leave the vacuum manifold only if

[2]This is an unproven conjecture, motivated, e.g., by observations of the density of textures and monopoles in liquid crystals and by numerical experiments [13,31].

it would otherwise be forced to gradients of order $(\nabla\phi)^2 \sim \lambda\phi^2\eta^2$, thus only over length scales of order $l = 1/(\sqrt{\lambda}\,\eta) \equiv m_\phi^{-1}$ (l is the transversal extension of the defects). For GUT scale phase transitions $l \sim 10^{-30}$ cm, where cosmic distances are of the order of Mpc $\sim 10^{24}$ cm. If we are willing to lose the information of the precise field configuration over these tiny regions, it seems well justified to fix ϕ to the vacuum manifold $\mathcal{N}$. Instead of discussing the field equation (28), we require $\phi/\eta \in \mathbf{S}^{(N-1)}$. The remaining field equation, $\Box\phi = 0$, then demands that

$$\phi/\eta \equiv \beta \;:\; \mathcal{M} \to \mathbf{S}^{(N-1)}$$

is a harmonic map from spacetime $\mathcal{M}$ into $\mathbf{S}^{(N-1)}$.

The topological defects we are interested in are singularities of these maps. When the gradients of ϕ become very large, such as, e.g., towards the center of a global monopole, the field leaves the vacuum manifold and assumes nonvanishing potential energy. If $\beta \in \mathbf{S}^{(N-1)}$ is enforced, a singularity develops by topological reasons.

In the physics literature, harmonic maps are known as σ models. The action of a σ model is given by

$$S_\sigma = \int_{\mathcal{M}} g^{\mu\nu}\partial_\mu\beta^A\partial_\nu\beta^B\gamma_{AB}(\beta)\sqrt{|g|}\,d^4x, \tag{29}$$

where γ_{AB} denotes the metric on $\mathbf{S}^{N-1}$ and $g_{\mu\nu}$ is the metric of spacetime. We fix β to lay in the vacuum manifold $\mathbf{S}^{N-1}$ by introducing a Lagrange multiplier. We then obtain the following equation of motion for β:

$$\Box\beta - (\beta\cdot\Box\beta)\beta = 0, \tag{30}$$

which shows that the σ model is scale free. There are thus two possible evolution equations for the scalar field at low temperature. We call Eq. (28) the ''potential model'' evolution equation and Eq. (30) the σ-model approach.

The energy-momentum tensor of the scalar field perturbs spacetime geometry and induces perturbations in the dark matter energy density according to Eq. (26):

$$\ddot{D} + \left(\frac{\dot{a}}{a}\right)\dot{D} - 4\pi G a^2\rho_C D = 8\pi G\dot{\phi}^2, \tag{31}$$

where D is a gauge-invariant variable for the dark matter perturbations [29]. On subhorizon scales $D \sim \delta\rho/\rho$. In comoving coordinates, the total perturbed energy-momentum tensor is given by

$$\delta T^\nu_\mu = \phi_{,\mu}\cdot\phi^{,\nu} - \frac{1}{2}\delta^\nu_\mu\phi_{,\lambda}\cdot\phi^{,\lambda} + \rho_C D\,\delta^0_\mu\delta^\nu_0.$$

As already mentioned in Sec. II, the perturbed Einstein equations to this energy momentum tensor yield an algebraic equation for the divergence of the electric part of the Weyl tensor and an evolution equation for the magnetic part of the Weyl tensor (see the Appendix):

$$\partial^j E_{ij} = -\frac{8\pi}{3}G\rho_C a^2 D_i - 8\pi G\left[\frac{1}{3}\partial_i\delta T_{00} + \left(\frac{\dot{a}}{a}\right)\delta T_{0i} + \frac{1}{2}\partial^j\tau_{ij}\right], \tag{32}$$

and

$$\frac{1}{a}(aB_{ij})^{\cdot\cdot} - \nabla^2 B_{ij} = 8\pi G\mathscr{S}^{(B)}_{ij}, \tag{33}$$

with

$$\mathscr{S}^{(B)}_{ij} = \epsilon_{lm(i}[T^S_{0l,j)m} + \dot{\tau}_{j)l,m}]$$

and

$$\tau_{ij} = \phi_{,i}\phi_{,j} - \frac{1}{3}\delta_{ij}(\nabla\phi)^2.$$

The source term for the perturbation of the Liouville equation is given by Eq. (24):

$$-3n^i\partial^j E^{(S)}_{ij} + n^k n^j\epsilon_{klj}\partial_l B^{(S)}_{ij} \equiv S_{ST}(t,\boldsymbol{x},\boldsymbol{n}). \tag{34}$$

The CMB fluctuations are then determined according to

$$\frac{\delta T}{T}(t,\boldsymbol{x},\boldsymbol{n}) = \int_{t_i}^{t} S_{ST}(t',\boldsymbol{x}+(t'-t)\boldsymbol{n},\boldsymbol{n})dt' + \Phi_S(t_i,\boldsymbol{x}+(t_i-t)\boldsymbol{n},\boldsymbol{n}) + \frac{1}{3}\Psi_C(t_i,\boldsymbol{x}_i) - \frac{2}{3}\dot{\Psi}_C/(\dot{a}/a)(t_i,\boldsymbol{x}_i) + 2\int_i^f\dot{\Psi}_C dt. \tag{35}$$

Equations (28) and (31)–(35) form a closed, hyperbolic system of partial differential equations. Actually, all except the scalar field equation (28), are linear perturbation equations with source terms. The differential equations for $\delta T/T$, D, and B_{ij} can thus be solved, e.g., by the Wronskian method, i.e., by some integrals over the source term. The corresponding solution for $\delta T/T$ is given in Eq. (35), the general solution of the dark matter equation is given below in Eqs. (45), (46), and (47).

Let us briefly describe the general solution for B_{ij}: We switch to Fourier space, because there the ∇^2 is a simple multiplication by $-k^2$ and Eq. (33) becomes an ordinary differential equation with scalar homogeneous solutions

$$b^\pm = \frac{1}{a}\exp(\pm ikt). \tag{36}$$

The general solution to the inhomogeneous equation is given by

$$B_{ij} = (b^+ C^+_{ij} + b^- C^-_{ij}) + B^{(hom)}_{ij}, \tag{37}$$

where B^{hom} denotes an arbitrary homogeneous solution and C^+, C^- are given by

$$C_{ij}^{+}=-8\pi G\int\frac{\tilde{\mathscr{T}}_{ij}^{(B)}b^{-}}{W}dt, \tag{38}$$

$$C_{ij}^{-}=8\pi G\int\frac{\tilde{\mathscr{T}}_{ij}^{(B)}b^{+}}{W}dt. \tag{39}$$

Here, W denotes the Wronskian determinant of the solutions which amounts to

$$W=b^{+}\dot{b}^{-}-b^{-}\dot{b}^{+}=\frac{2ik}{a^{2}}. \tag{40}$$

IV. INITIAL CONDITIONS AND NUMERICAL METHODS

A. The scalar field

As already shown in the previous section, the equation of motion of the scalar field is given by

$$g^{\mu\nu}\nabla_{\mu}\nabla_{\nu}\phi+\frac{\partial V}{\partial\phi}=0, \tag{41}$$

where $g^{\mu\nu}$ is the background (unperturbed metric). With $\beta=\phi/\eta$ and $m=\sqrt{\lambda}\,\eta$, Eq. (41) yields, for O(N) models in a Friedmann universe,

$$\partial_{t}^{2}\beta+2(\dot{a}/a)\partial_{t}\beta-\nabla^{2}\beta=\frac{1}{2}a^{2}m^{2}(\beta^{2}-1)\beta. \tag{42}$$

This equation as it stands cannot be treated numerically in the regime which is interesting for large-scale structure formation. The two scales in the problem are the horizon scale $t\sim(\dot{a}/a)^{-1}$ and the inverse symmetry-breaking scale, the comoving scale $(am)^{-1}$. At recombination, e.g., these scales differ by a factor of about 10^{53} and thus both cannot be resolved in one computer code.

There are two approximations to treat the scalar field numerically. As we shall see, they are complementary and thus the fact that both approximations agree with each other within about 10% is reassuring. The first possibility is to replace $(am)^{-1}$ by w, the smallest scale which can be resolved in a given simulation, typically twice the grid spacing, $w\sim2\Delta x$. The time dependence of $(am)^{-1}$ which results in a steepening of the potential is mimicked by an additional damping term: $2(\dot{a}/a)\rightarrow\alpha\dot{a}/a$, with $\alpha\sim3$ [32]. Numerical tests have shown that this procedure, which usually is implemented by a modified staggered leap frog scheme [33], is not very sensitive on the values of α and w chosen. With this method, we have replaced the growing comoving mass am by the largest mass which our code can resolve. For a $(256)^{3}$ grid which simulates the evolution of the scalar field until today, we obtain $256\Delta x\sim t_{0}\sim4\times10^{17}$ sec$/a_{0}$, so that $w\sim4\times10^{15}$ sec$/a_{0}$, i.e., $am\sim\eta a_{rec}\sim10^{17}$ GeV is replaced by about $w^{-1}=a_{0}10^{-39}$ GeV $\sim10^{-35}$ GeV, where we set $a_{eq}=1$.

We are confident that this modified equation mimics the behavior of the field, since the actual mass of the scalar field is irrelevant as long as it is much larger than the typical kinetic and gradient energies associated with the field which are of the order of the inverse horizon scale. Therefore, as soon as the horizon scale is substantially larger than Δx, the code should mimic the true field evolution on scales larger than w. But, to our knowledge, there exists no rigorous mathematical approximation scheme leading to the above treatment of the scalar field which would then also yield the optimal choice for α.

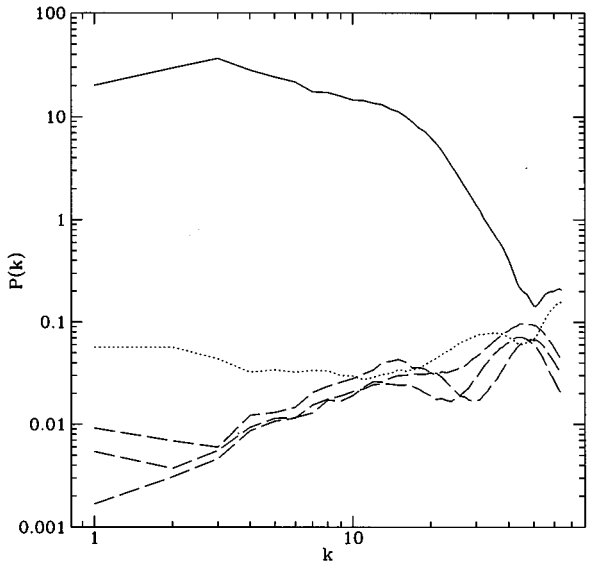

FIG. 2. The quantities $|(T_{0}^{\mu};_{\mu})|^{2}$ (dotted line), $|(T_{i}^{\mu};_{\mu})|^{2}$ (dashed lines) and $|(T_{0}^{0}/t)|^{2}$ (solid line) are shown as functions of k. The inaccuracy in energy- and momentum-conservation is below 10% for $k\leqslant32=128/4$. This hints that our code is accurate to better than 10% for wavelengths of four grid spacings and larger.

Alternatively, we can treat the scalar field in the σ-model approximation given in the previous section. This approach is opposite to the one outlined above in which the scalar field mass is much too small, since the σ model corresponds to setting the scalar field mass equal infinity.

The σ-model equation of motion cannot be treated numerically with a leap frog scheme, since it involves nonlinear time derivatives. In this case, a second-order accurate integration scheme has been developed by varying the discretized action with respect to the field [18].

The two different approaches have been extensively tested by us and other workers in the field, and good agreement has been found on scales larger than about 3–4 grid sizes [34,35]. We have compared our potential code with the exact spherically symmetric scaling solution [36] and with our old spherically symmetric σ-model code [19]. Outside the unwinding events which extend over approximately three grid sizes, the different approaches agree within about 5%. This is very encouraging, especially since the two treatments are complementary: In the σ model, we let the scalar field mass m go to infinity. In the potential approach, we replace m by $\sim1/\Delta x\sim200/t_{0}\sim200a_{0}/10^{10}y\sim10^{-35}$ GeV.

The integration of the scalar field equation is numerically the hardest part of the problem, since it involves the solution of a system of nonlinear partial differential equations. A good test of our numerical calculations, next to checking the scaling behavior of ρ_{S}, is energy-momentum conservation of the scalar field, $T_{;\nu}^{(S)\mu\nu}=0$. Energy-momentum conservation in the potential model, with about 15% accuracy, is slightly worse than in the σ model, where it is about 5% accurate

(see Fig. 2). Therefore, the final results presented here are all obtained with the σ-model approach. Our checks lead us to the conclusion that we can calculate the scalar field energy-momentum tensor, which then is the source of dark matter and CMB fluctuations, to an accuracy of about 10%. The problem of choosing the correct initial condition may induce another (systematical) error in our calculations which we hope to remain below 20%. Other sources of error are negligible.

B. Dark matter

Once the scalar field $\beta(\boldsymbol{x},t)$ is known, the dark matter perturbations can easily be calculated by either using the Wronskian method (see below) or some standard ordinary differential equation solver. We have performed both methods and they agree very well. For later use, we briefly describe the Wronskian method. We normalize the scale factor by

$$a=\frac{t}{\tau}(1+\tfrac{1}{4}t/\tau),$$

with

$$\tau=1/\sqrt{(4\pi G/3)\rho_{\rm eq}}=\frac{t_{\rm eq}}{2(\sqrt{2}-1)}.$$

Here, $t_{\rm eq}$ denotes the time of equal matter and radiation density, $\rho_{\rm rad}(t_{\rm eq})=\rho_C(t_{\rm eq})=(1/2)\rho(t_{\rm eq})$. We have normalized a such that $a_{\rm eq}=a(t_{\rm eq})=1$. Transformed to the variable a, the dark matter equation (26) then yields

$$\frac{d^2D}{da^2}+\frac{2+3a}{2a(1+a)}\frac{dD}{da}-\frac{3}{2a(1+a)}D$$
$$=2\epsilon\dot{\beta}^2\left(\frac{da}{dt}\right)^2=(1+a)S/\tau^2, \tag{43}$$

$$S=2\epsilon\dot{\beta}^2 \quad \text{and} \quad \epsilon=4\pi G\eta^2.$$

The homogeneous solutions to this linear differential equation are well known [37]:

$$D_1=1+\frac{3}{2}a, \tag{44}$$

$$D_2=\left(1+\frac{3}{2}a\right)\left[\ln\left(\frac{\sqrt{a+1}+1}{\sqrt{a+1}-1}\right)-3\sqrt{a+1}\right]. \tag{45}$$

The general solution to Eq. (43) is given by

$$D(t)=c_1(t)D_1(t)+c_2(t)D_2(t) \tag{46}$$

with

$$c_1=-\int (SD_2/W)dt, \quad c_2=\int (SD_1/W)dt,$$

$$W=D_1\dot{D}_2-\dot{D}_1D_2=\frac{\dot{a}(1+\frac{3}{2}a)^3}{a\sqrt{a+1}}=\frac{(1+\frac{3}{2}a)^3}{a\tau} \tag{47}$$

is the Wronskian determinant of the homogeneous solutions. The integrals [Eq. (47)] have to be performed numerically with $S=\epsilon\dot{\beta}^2$. When discussing the initial conditions for D in Sec. IV D, we shall present an analytic approximation for the source term S.

C. The CMB anisotropies

The CMB anisotropies are given by

$$\frac{\delta T}{T}=\nabla^{-2}\chi$$

up to monopole and dipole contributions which we disregard. Here, χ is a solution of Eq. (18). The source term S_T is determined via Eqs. (25) and (27). However, using this straightforward approach results in a big waste of computer memory (which we cannot afford): We would be satisfied to calculate $\delta T/T$ for about 30 observers in each simulations, which means we need $\nabla^{-2}\chi$ only at 30 positions $\mathbf{x}$. But since we have to perform an inverse Laplacian which is done by fast Fourier transforms, we have to calculate χ on the whole grid, which consists of $192^3\sim 7\times 10^6$ positions. In addition, to calculate the spherical harmonic amplitudes of $\delta T/T$ up to about $l\sim 40$ (angular resolution of about 4°), we need typically 5×10^4 directions $\boldsymbol{n}$. The χ variable alone (in double precision) would thus require 700 Gbytes of memory, an amount which is not available on present-day computers. The way out is to take the inverse Laplacian already in the equation of motion (18). This results in

$$(\partial_t+\gamma^i\partial_i)\frac{\delta T}{T}=-3\gamma^i\nabla^{-2}(\partial^j E_{ij})-\gamma^k\gamma^j\epsilon_{kli}\nabla^{-2}(\partial_l B_{ij})$$
$$\equiv\nabla^{-2}S_T(t,\boldsymbol{x},\gamma). \tag{48}$$

Here, the inverse Laplacian has to be performed for a vector field and a symmetric traceless tensor field, a total of eight scalar variables which only depend on $\mathbf{x}$ and not on γ. For a 192^3 grid, the total code then reaches a size of about 1 Gbyte of memory, no problem for presently available machines. Equation (48) has the general solution [see Eq. (23)]

$$\frac{\delta T}{T}(t_0,\boldsymbol{x}_0,\gamma)=+\Phi_S(t_i,\boldsymbol{x}_i)$$
$$-\int_i^f\nabla^{-2}S_{TS}(t,\boldsymbol{x}_0-(t_f-t)\boldsymbol{n},\boldsymbol{n})dt$$
$$+\frac{1}{3}\Psi_C(t_i,\boldsymbol{x}_i)-\frac{2}{3}\dot{\Psi}_C/(\dot{a}/a)(t_i,\boldsymbol{x}_i)$$
$$+2\int_i^f\dot{\Psi}_C dt, \tag{49}$$

with S_{TS} given in Eq. (24). Here, vector perturbations of the dark matter [which are not seeded by the defects, see Eq. (26), and thus decay quickly] are neglected. The first term of Eq. (49) determines the initial condition of the CMB anisotropies caused by the source. In the numerical simulation, we just set it $-3n^l\nabla^{-2}(\partial^j E^{(S)}_{lj})(t_i,\boldsymbol{x}_i)t_i$. This assumes that the source term is approximately constant until t_i and

that magnetic contributions can be neglected. The resulting amplitude is not very sensitive to this assumption, but changing it can somewhat influence the spectral index. We have solved Eq. (49) numerically by just summing up the contributions from each time step for 27 observer positions $\boldsymbol{x}_0$. The value of the source term at position $\boldsymbol{x}_0+(t-t_0)$ is determined by linear interpolation. The quantity $\partial^i E^S_{ij}$ is determined by Eq. (25) and its inverse Laplacian is calculated by fast Fourier transforms. To obtain $\nabla^{-2}B^S_{ij}$ from Eq. (27), we directly calculate $\nabla^{-2}S^{(B)}$ in k-space, then solve the ordinary, linear differential equation for $\nabla^{-2}B_{ij}$ in k-space by the Wronskian method. Since all components $T^{(S)}_{\mu\nu}$ in average scale such as $A/\sqrt{t}$ on superhorizon scales, $\mathscr{S}^{(B)}\sim At^{-1/2}$ and therefore $C^{\pm}\propto t^{5/2}$ on superhorizon scales. Therefore, we can neglect the contribution to $C^{\pm}$ from the lower boundary in the integral. Furthermore, since the homogeneous solution $B^{(\mathrm{hom})}_{ij}$ is decaying, we drop it entirely. This procedure corresponds to setting $B(t_i)=0$ and calculating $B(t)$ according to Eq. (37).

D. Initial conditions

Initially, the field ϕ itself and/or the velocities $\dot{\phi}$ are laid down randomly on the grid points. The initial time t_{in} is chosen to be the grid size $t_{\mathrm{in}}=\Delta x$, so that the field at different grid points should not be correlated. The configuration is then evolved in time with one of the approximation schemes discussed above.

Because our initial conditions for dark matter and photons very sensitively depend on the scaling behavior of the scalar field (see below), we can only start the dark matter or photon simulations when scaling is fully reached, $t_{in}=8\Delta x$. Starting our simulations, e.g., at $t=4\Delta x$, changes the results by about a factor of 2. Further doubling of the initial time, changes our results by less than 20%, we thus believe that at $t=8\Delta x$ scaling is sufficiently accurate. Unfortunately, this late initial time reduces our dynamical range to about $192/8=24$ for a 192^3 grid, which is seen clearly in our results for the CMB anisotropies discussed below.

It is very important to choose the correct initial conditions for the dark matter and the photon perturbations induced by the dark matter. Changing them can change the CMB fluctuation amplitudes by more than a factor of 2. Since these fluctuations are used to normalize the model, i.e., to determine ϵ, this reflects in corresponding changes in ϵ. We want to do better than a factor of 2 by choosing physically plausible initial conditions. The cleanest way would be to simulate the evolution of perturbations through the phase transition, assuming that before the phase transition, the universe was an unperturbed Friedmann universe with $\phi\equiv 0$. On the other hand, since we want to calculate the perturbation spectrum on scales of up to 1000 Mpc with a $(256)^3$ grid, we cannot start our dark matter and CMB simulation earlier than at a time when the horizon distance is approximately $8\Delta x\sim 30$ Mpc. At the beginning of the scalar field simulation, our grid scale $\Delta x\sim 4$ Mpc is of the order of the horizon scale. We therefore have to decide on the amplitudes of superhorizon perturbations. One possibility is setting all geometrical perturbations initially to zero. The requirements

$$\partial^j E_{ij}(t_i)=0 \quad \text{and} \quad \mathscr{S}^{(B)}_{ij}(t_i)=0$$

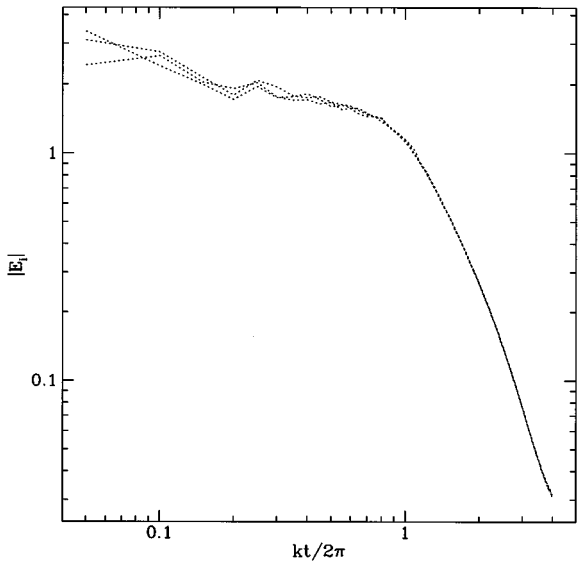

FIG. 3. The spectrum of the electric part of the Weyl tensor as a function of kt at time $t=8$ for a grid of size 160. On large scales, $kt/(2\pi)<1$, the spectrum is flat, white noise.

then yield initial conditions for the dark matter fluctuations D and the photon variable χ. But these, let us call them ''strict isocurvature'' initial conditions, are not natural since they do not propagate in time: Even if we start with E and B vanishing on superhorizon scales, after some time residual fluctuations have leaked into these scales and one obtains the white noise fluctuations spectrum on superhorizon scales shown in Fig. 3. This does not violate causality, since white noise is uncorrelated and just results from the residuals of correlated fluctuations on smaller scales. The correct initial values for D and $\dot{D}$ would, of course, be those obtained by solving the equation of motion Eq. (26) from the symmetry-breaking time until the start of the simulation. We found a method to incorporate this at least approximately: The spectrum of the dark matter source term $8\pi G|\widetilde{\dot{\phi}^2}|^2$ can be approximated by

$$8\pi G|\widetilde{\dot{\phi}^2}|=2\epsilon\widetilde{\dot{\beta}^2}=\epsilon\sqrt{\frac{1}{V}}\int d^3x\dot{\beta}^2(x)e^{ikx}$$

$$\approx\frac{\epsilon A}{\sqrt{t}[1+a_1kt+a_2(kt)^2]}, \tag{50}$$

with

$$A=3.3, \quad a_1=-0.7/(2\pi), \quad a_2=0.7/(2\pi)^2.$$

These numbers have been obtained by a χ^2–minimization scheme. The approximation is not very good. It yields a $\chi^2\approx 2000$ for about 1000 data points. Its comparison with the real data in Figs. 4 and 5 shows that Eq. (50) approximates the source term to about 10% on superhorizon scales, but does not follow the wiggles present in the data on smaller scales. Since we shall not use the fit on subhorizon scales, this is not important for our simulations. However, in general, $\widetilde{\dot{\phi}^2}$ is complex and setting it equal to its absolute value,

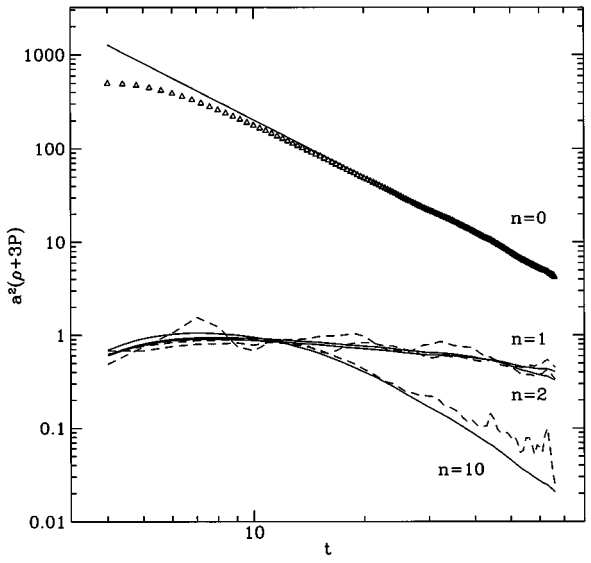

FIG. 4. The dashed curves and the triangles show $\dot{\beta}^2$ as a function of t for fixed values of $k=n/n_{\rm tot}$ for $n_{\rm tot}=128$. The solid lines show the fits according to the fitting formula given in the text.

we neglect the evolution of phases. Again, by causality, this will not severely affect scales larger than the horizon, since on these scales the phases are (approximately) frozen. But on subhorizon scales, our fit is not very useful because the incoherent evolution of phases. Assuming this form of the source term, we can solve Eq. (26) analytically on superhorizon scales, where we approximate the source term by

$$2\epsilon\widetilde{\dot{\beta}^2}=\frac{\epsilon A}{\sqrt{t}}, \quad \text{on superhorizon scales.} \tag{51}$$

The homogeneous solutions of Eq. (26) are given by Eqs. (44) and (45). The general inhomogeneous solution,

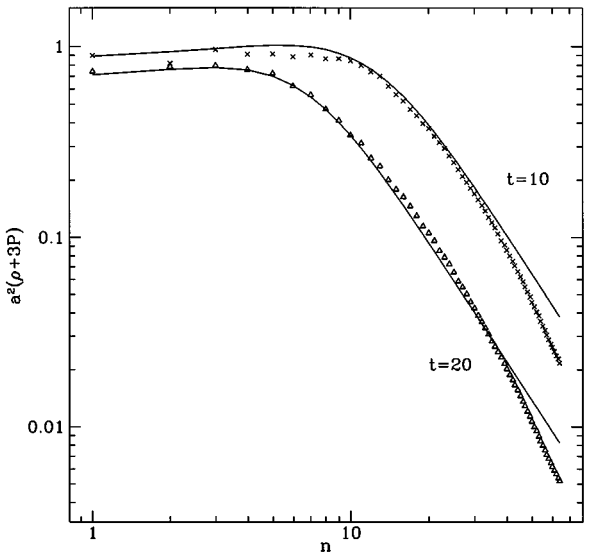

FIG. 5. The crosses and triangles show $\dot{\beta}^2$ as a function of n, with $k=n/n_{\rm tot}$ for fixed values of t. The solid curves show the fits according to the fitting formula given in the text.

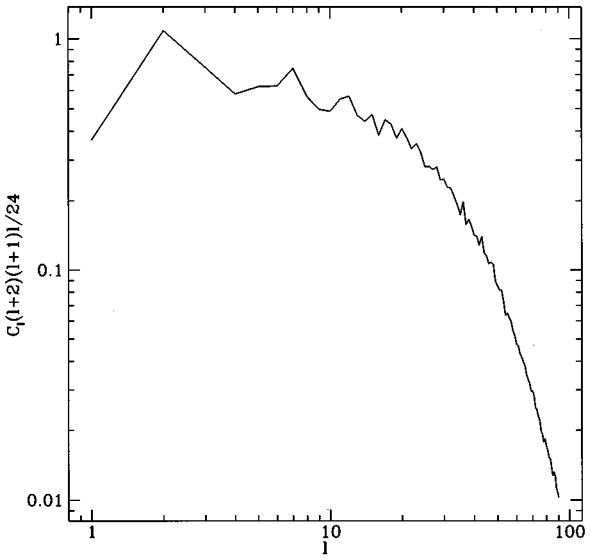

FIG. 6. The dark matter contribution to the C_ℓ's from a $(160)^3$ simulation. $(\ell+2)(\ell+1)\ell C_\ell/24$ is shown. For $\ell<20$, which is the dynamic range of this simulation, a white noise, $n=0$, spectrum fits reasonably well.

$D=c_1D_1+c_2D_2$, even with the simple source term equation (51), becomes rather complicated. But in the radiation- and matter-dominated regimes, we find the simple approximations

$$D=(4/7)t^2S; \quad \dot{D}=(6/7)t^2S \ \text{ radiation dominated,} \tag{52}$$

$$D=-(4/9)t^2S; \quad \dot{D}=-(2/3)t^2S \ \text{ matter dominated.} \tag{53}$$

From D we can calculate Ψ_C, leading to the dark matter contribution to the CMB anisotropies.

As mentioned above, the initial contribution of the scalar field is approximated by

$$\Phi^S(t_i,\boldsymbol{x}_i)\sim -3t_i n^i\nabla^{-2}(\partial^j E_{ij}^{(S)}).$$

The result does not depend very strongly on this initial condition, however, it is very sensitive to the *dark matter* initial conditions: If we choose some arbitrary, nonadiabatic initial condition, the resulting C_ℓ's increase by nearly a factor of 10 and the dark matter induces 80% of the total fluctuation. Choosing adiabatic initial conditions as discussed in Sec. III, leading to Eq. (49), dark matter only contributes about 20% to the angular power spectrum and the main contribution is because of the defects. The dark matter contribution to the CMB anisotropies is not scale invariant, but is white noise. It has a spectral index $n=0$. This result was found numerically (see Fig. 6) but it is also clear from Eq. (50) which shows again that on superhorizon scales $\dot{\phi}^2$ and therefore also D have white noise spectra.

Our value of ϵ obtained with these physical isocurvature and on superhorizon scale adiabatic initial conditions, is in reasonable agreement with the values obtained in [18] and [17].

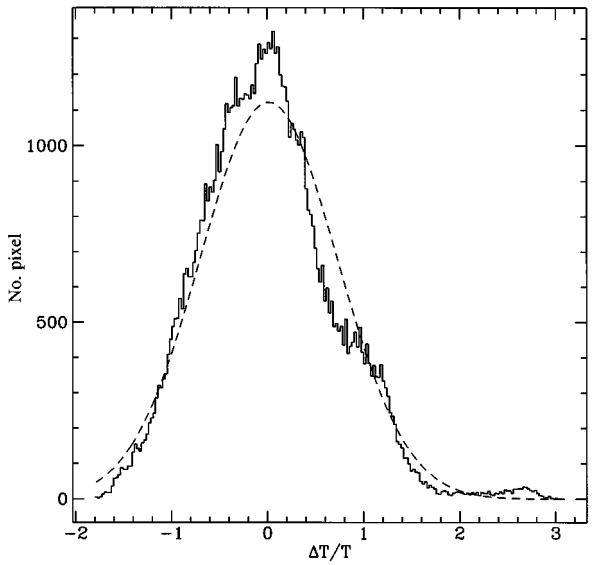

FIG. 7. The pixel distribution of $\delta T/T$ for one observer.

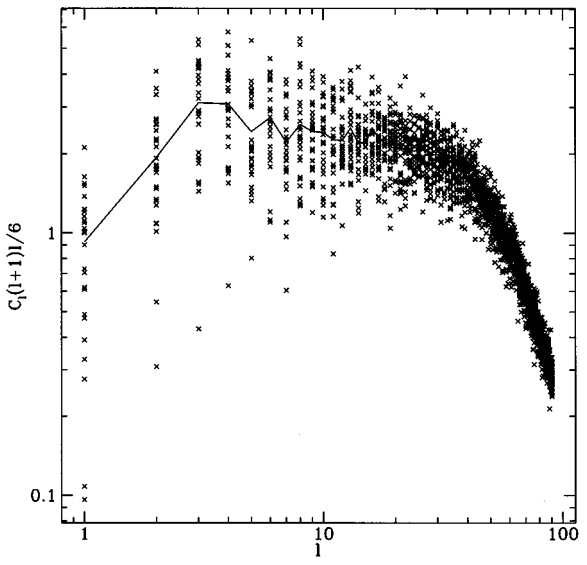

FIG. 8. The values $\ell(\ell+1)C_\ell/6$ for 27 observers are plotted for $\epsilon=1$. The crosses are the individual observers and the solid line indicates the average. The sharp drop after $\ell\sim 30$ is because of finite resolution (our dynamical range is approximately 25).

Let us also present a heuristic derivation of the numerical finding equation (51) on superhorizon scales: We know that the average value $\langle\dot\beta^2\rangle\propto 1/t^2$, the usual scaling behavior. The Fourier transform of $\dot\beta^2$ determines the fluctuations on this ''background'' on a given comoving scale $\lambda=2\pi/k$. As long as this scale is superhorizon, $\lambda>t$, a patch of size λ^3 consists of $N=(\lambda/t)^3$-independent horizon size volumes. The fluctuations on this scale should thus be proportional to

$$\widetilde{\dot\beta^2}\propto\langle\dot\beta^2\rangle/\sqrt{N}\propto 1/\sqrt{t},$$

which is just the behavior which we have found numerically on superhorizon scales.

As soon as a given scale becomes subhorizon, $\lambda\ll t$, $\widetilde{\dot\beta^2}$ starts decaying from this large scale value proportional to $1/t^2$.

V. RESULTS

A. CMB anisotropies

To analyze the CMB anisotropies, we expand $\delta T/T$ in spherical harmonics

$$\frac{\delta T}{T}(t_0,\boldsymbol{x},\gamma)=\sum_{lm} a_{lm}(\boldsymbol{x})Y_{lm}(\gamma). \tag{54}$$

As usual, we assume that the average over N_x different observer positions coincides with the ensemble average (a kind of ''ergodic hypothesis''). We define

$$C_\ell=\frac{1}{(2\ell+1)N_x}\sum_{m,x}|a_{\ell m}(\boldsymbol{x})|^2,\quad \ell\geqslant 2. \tag{55}$$

Gaussian fluctuations are characterized by the two-point correlation function. Since the angular two-point correlation function is given by

$$\left\langle\frac{\delta T}{T}(\boldsymbol{n})\frac{\delta T}{T}(\boldsymbol{n}')\right\rangle_{(\boldsymbol{n}\cdot n'=\cos\theta)}=\frac{1}{4\pi}\sum_\ell(2\ell+1)\times C_\ell P_\ell(\cos\theta), \tag{56}$$

Gaussian-distributed CMB fluctuations are fully determined by the C_ℓ's. However, as can be seen from Fig. 7, in our case the distribution of the CMB fluctuations is not quite Gaussian. It is slightly negatively skewed. We find an average skewness of -0.5 and a kurtosis of 0.7. In Fig. 8 we show the harmonic amplitudes for five simulations on a 192^3 grid with 27 different observer positions for each simulation. The low-order multipoles depend strongly on the random initial conditions (cosmic variance), as was found in the spherically symmetric simulation [19].

It is well known that cold dark matter fluctuations with a power spectrum of spectral index n gravitationally induce CMB anisotropies with a spectrum given by [38]

$$C_\ell=C_2\frac{\Gamma(l+(n-1)/2)\Gamma((9-n)/2)}{\Gamma(l+(5-n)/2)\Gamma((n+3)/2)}. \tag{57}$$

We have performed a least square fit of $\log_{10}(C_\ell)$ from our numerical results fitted with $\log_{10}(C_\ell)$ obtained from Eq. (57).[3] If we take into account all the C_l's reliably calculated in our simulations, which limits us approximately to $l\leqslant 22$, we find a very nice scale-invariant spectrum,

$$n=0.9\pm 0.2, \tag{58}$$

[3]In the case of topological defect-induced fluctuations, the C_ℓ spectrum does not have precisely this form, since CMB fluctuations are not only induced by the dark matter but mainly by the scalar field perturbations and the assumptions made for the derivation of this formula are not valid.

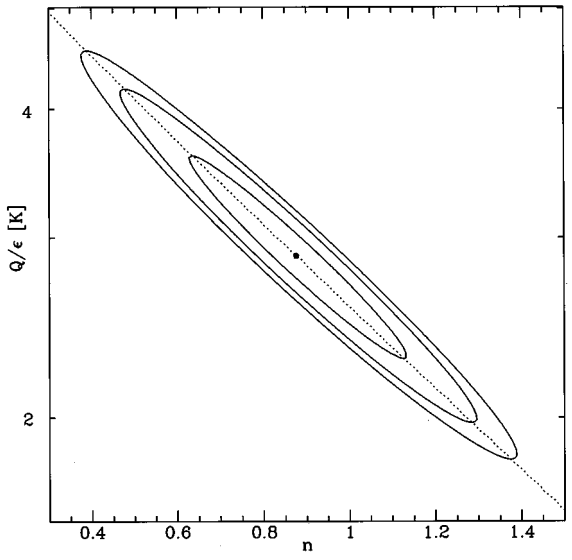

FIG. 9. The χ^2 contour plots for 66%, 95%, and 99% confidence levels from fitting the C_ℓ, to a spectrum with index n with quadrupole amplitude Q according to Eq. (57) for $\ell \leqslant 20$. In total, 81 observers from three different $(192)^3$ simulations have been taken into account.

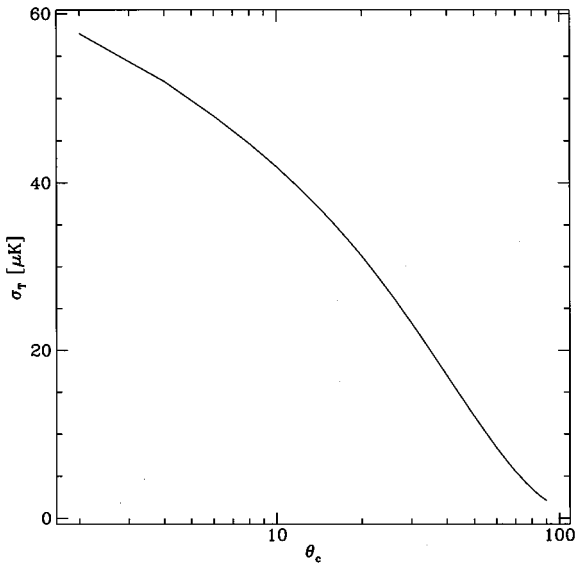

FIG. 10. The root mean square of the temperature fluctuation at given angular scale is shown as a function of angle for $\epsilon = 10^{-5}$.

with quadrupole amplitude

$$Q = \sqrt{(5/4\pi)C_2}\,T_{\rm CMB} = (2.8 \pm 0.7) K \cdot \epsilon. \tag{59}$$

The 1, 2, and 3 sigma contour plot is shown in Fig. 9. The minimal χ^2 is 0.56.

It is very interesting that the dark matter contribution to the CMB anisotropies does not yield a scale-invariant spectrum, but white noise. This can be understood analytically: The $\dot{\Psi}_C$ contributions to $\delta T/T$ in Eq. (23) are not very important and

$$(\delta T/T)_C(t_0, \boldsymbol{k}) \sim \frac{1}{3}\Psi_C(t_i, \boldsymbol{k}) \exp(i\boldsymbol{k}\cdot n t_0)$$

$$= \frac{\epsilon A}{6\sqrt{t_i}} \frac{\exp(i\boldsymbol{k}\cdot n t_0)}{k^2}$$

on superhorizon scales. For the second equal sign, we used $k^2\Psi_C = 4\pi G D_C \sim \epsilon A/2\sqrt{t_i}$. By standard arguments (see, e.g., [38]), one then finds

$$C_\ell^{(C)} = \frac{\epsilon^2 A^2}{18\pi t_i} \int \frac{dk}{k^2} j_\ell^2(kt_0) \propto \frac{\Gamma(\ell - 0.5)}{\Gamma(\ell + 2.5)}, \tag{60}$$

corresponding to Eq. (57) with $n = 0$. This is also what we find numerically (see Fig. 6). The dark matter contribution caused the spectral index n of the total CMB anisotropies to drop slightly below $n = 1$.

To reproduce the COBE amplitude $Q_{\rm COBE} = (20 \pm 5)\mu K$, [14] we have to normalize the spectrum by choosing the phase transition scale η according to

$$\epsilon = 4\pi G \eta^2 = (0.8 \pm 0.4) \times 10^{-5}. \tag{61}$$

This value is somewhat smaller, but still comparable with the results obtained in [17,18]. But even taking into account the considerable uncertainties, the difference of nearly a factor of 2 between the result (61) and Refs. [17,18] (normalized to the two-year COBE data) is somewhat disturbing and deserves future investigation.

Another method to determine ϵ is the following: The total temperature fluctuation amplitude on a given angular scale θ_C is given by

$$\sigma_T^2(\theta_C) = \frac{1}{4\pi} \sum_\ell C_\ell (2\ell + 1) \exp(-\ell^2 \theta_C^2/2). \tag{62}$$

In Fig. 10 we show σ_T as a function of θ_C. In a recent analysis of the COBE data [40] $\sigma_T^{(\rm COBE)}(7^\circ) \sim 44\ \mu K$ and $\sigma_T^{(\rm COBE)}(10^\circ) \sim 40\ \mu$K for a spectral index $n \sim 1$, which leads again to the result given in Eq. (61).

B. Dark matter fluctuations

Using fast Fourier transforms, we calculate the spectrum $P(k) = |\delta(k)|^2$ of the dark matter density fluctuations as shown in Fig. 11. The fit represented as dashed line in Fig. 11 is given by

$$P(k) h^3/(2\pi)^3 = \frac{Ck}{[1 + \alpha k + (\beta k)^{1.5} + (\gamma k)^2]^2}, \tag{63}$$

with $h = 0.5$ and

$$C = 215 h^{-1}\ {\rm Mpc}^4, \tag{64}$$

$$\alpha = 10 h^{-2}\ {\rm Mpc}\ \ (= 0.5\tau), \tag{65}$$

$$\beta = 1.25 h^{-2}\ {\rm Mpc}\ \ \sim \tau/(4\pi), \tag{66}$$

$$\gamma = 2.3 h^{-2}\ {\rm Mpc}\ \ \sim \tau/(2\pi), \tag{67}$$

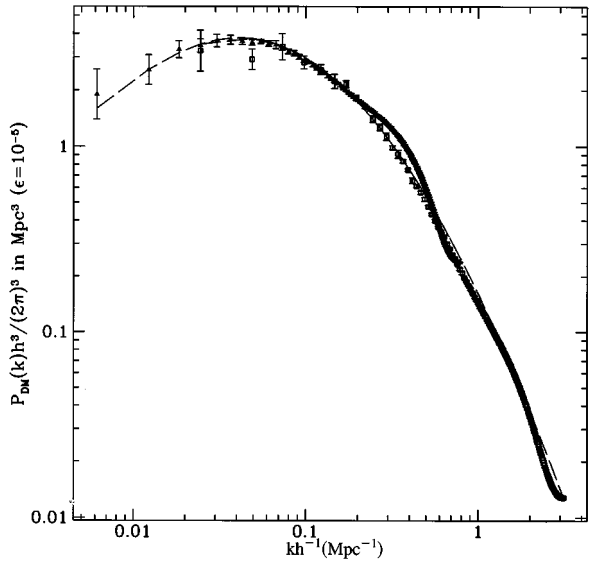

FIG. 11. The dark matter power spectrum (without bias and nonlinear evolution). The result is averaged over 15 simulations on $(256)^3$ grids of two different physical scales. The error bar indicates one standard deviation. The dashed line shows the fit given in the text.

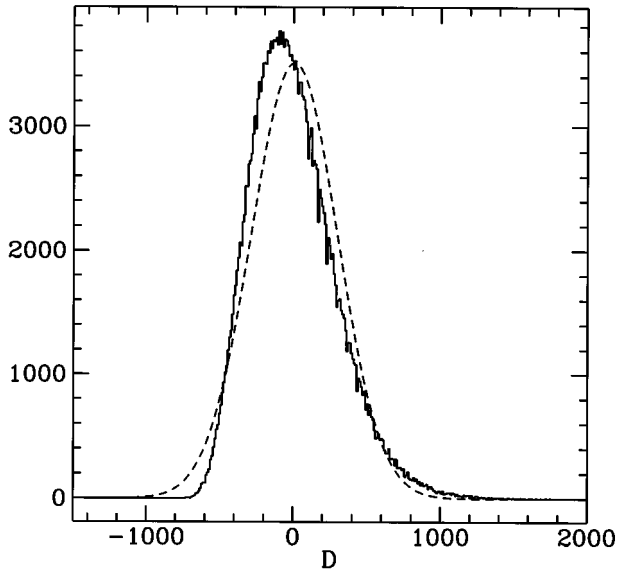

FIG. 12. The dark matter pixel distribution from linear perturbation theory. The positive skewness (0.76) and positive kurtosis (1.2) are clearly visible.

where we have used $\tau=19.36h^{-2}$ Mpc, which is approximately the comoving time at equal matter and radiation.

The parameter C, which is most important to determine the bias factor, can also be obtained by the following rough analytical argument, valid in the relevant, matter-dominated era: On superhorizon scales, $|D|^2\sim(0.5\epsilon A)^2t^3$ according to Eq. (53). As soon as the perturbation enters the horizon at $t=2\pi/k$, the source term disappears and D starts growing as t^2, leading to

$$P(k,t_0)\sim\frac{(0.5\epsilon A)^2}{2\pi}kt_0^4=\frac{(2\pi)^3}{h^3}C_{an}k. \tag{68}$$

Inserting the numbers $\epsilon=0.8\times10^{-5}$, $A=3.3$, $t_0^2=4a_0\tau^2$, $a_0\sim2.5h^2\times10^4$, we obtain $C_{an}\sim190h^{-1}$ Mpc^4 in excellent agreement with Eq. (64). Figure 11 can be compared directly with the Infrared Astronomy Satellite (IRAS) observation [39] and it is compatible with a bias factor of order 1. A more detailed calculation with Gaussian or square hat window function yields, for $\epsilon=0.8\times10^{-5}$,

$$\sigma_{\rm sim}(10\ \ {\rm MPc})=1/b_{10}\sim0.5-1$$

$$\sigma_{\rm QDOT}(10\ \ {\rm MPc})=1\ \ \text{for}\ \ h=0.5, \tag{69}$$

yielding $b_{10}\sim1-2$ for the value of ϵ found by comparison with COBE, Eq. (61). A value even somewhat closer to 1 is found for b_{20}. Observations and simulations of nonlinear clustering of dark matter and baryons [41] suggest a bias factor $b_{10}\sim1-2$ which is compatible with our results. It is remarkable that unlike in the simulations by Pen *et al.* [18], our bias factor is approximately constant and physically acceptable. (To determine our power spectrum, we have not taken into account any smoothing which might change the results by at most 15%.) In Fig. 12 we have shown the dark matter pixel distribution from a 100^3 simulation. It is interesting that the skewness of the dark matter distribution is positive, where the $\delta T/T$ skewness is negative.

VI. CONCLUSIONS

We have derived a new local, gauge-invariant cosmological perturbation equation for the treatment of free massless particles in a perturbed Friedmann universe. The gravitational field enters in this equation only via the Weyl curvature which is geometrically very satisfactory. We have applied this equation to determine the CMB anisotropies in the texture scenario of structure formation.

Our simulations show that global texture leads to a scale-invariant spectrum of microwave background fluctuations on large scales, such as inflationary models of structure formation. This is one of the main results of this investigation. However, the dark matter contribution to the CMB anisotropies is not scale invariant, but is white noise. It is important that the initial conditions for dark matter and radiation are adiabatic in which case the dark matter contribution to the C_ℓ's is small and the flat spectrum caused by the defects is maintained.

Our second main result is the dark matter fluctuation spectrum. The spectrum is very close to scale invariant and the bias factor needed for ϵ normalized by the CMB anisotropies is around $b\sim1-2$. As already mentioned, we have neglected radiation-density perturbations in our calculations. These lead to some additional damping of the dark matter perturbations on scales smaller than t_{rec}. The bias factor can be somewhat enhanced by this effect. However, the resulting value is certainly acceptable and smaller than the bias factor obtained in previous investigations [18].

The deviation from Gaussian statistics seems to us not very significant (see Figs. 7 and 12) and it is thus important to develop other means to distinguish topological defects from inflationary scenarios. A clean and promising candidate for this distinction are the Doppler peaks which are calcu-

lated for the texture scenario in [43].

From our investigations we thus conclude that, concerning the large scale CMB anisotropies and the linear dark matter perturbation spectrum, the texture scenario and probably also other models with global defects are compatible with present observations.

ACKNOWLEDGMENTS

We thank the staff at CSCS for valuable support. Especially, we want to mention Andrea Bernasconi, Djiordic Maric, and Urs Meier. We thank also Joachim Laukenmann who carefully read the manuscript and checked the more involved algebraic derivations with MAPLE. We profited from many helpful and encouraging discussions of this work, especially we want to mention Mark Hindmarsh, Philipp Jetzer, Yipeng Jing, Mairi Sakellariadou, Norbert Straumann, Neil Turok, Simon White, and others. We also thank Neil Turok for providing us their σ-model code. This work was partially supported by the Swiss National Science Foundation.

APPENDIX: THE EQUATION OF MOTION FOR THE MAGNETIC PART OF THE WEYL TENSOR

The Weyl tensor of a spacetime $(\mathcal{M},g)$ is defined by

$$C^{\mu\nu}{}_{\sigma\rho}=R^{\mu\nu}{}_{\sigma\rho}-2g^{[\mu}{}_{[\sigma}R^{\nu]}{}_{\rho]}+\frac{1}{3}Rg^{[\mu}{}_{[\sigma}g^{\nu]}{}_{\rho]}, \quad \text{(A1)}$$

where $[\mu,\ldots,\nu]$ denotes antisymmetrization in the indices μ and ν. The Weyl curvature has the same symmetries as the Riemann curvature and it is traceless. In addition, the Weyl tensor is invariant under conformal transformations:

$$C^{\mu}{}_{\nu\sigma\rho}(g)=C^{\mu}{}_{\nu\sigma\rho}(a^2g).$$

(Careful: This equation only holds for the given index position.) In four-dimensional spacetime, the Bianchi identities together with Einstein's equations yield equations of motion for the Weyl curvature. In four dimensions, the Bianchi identities

$$R_{\mu\nu[\sigma\rho;\lambda]}=0$$

are equivalent to [23]

$$C^{\alpha\beta\gamma\delta}{}_{;\delta}=R^{\gamma[\alpha;\beta]}-\frac{1}{6}g^{\gamma[\alpha}R^{;\beta]}. \quad \text{(A2)}$$

This, together with Einstein's equations, yields

$$C^{\alpha\beta\gamma\delta}{}_{;\delta}=8\pi G(T^{\gamma[\alpha;\beta]}-\tfrac{1}{3}g^{\gamma[\alpha}T^{;\beta]}), \quad \text{(A3)}$$

where $T_{\mu\nu}$ is the energy-momentum tensor, $T=T^{\lambda}_{\lambda}$.

Let us now choose some timelike unit vector field u, $u^2=-1$. We then can decompose any tensor field into longitudinal and transverse components with respect to u. We define

$$h^{\mu}{}_{\nu}\equiv g^{\mu}{}_{\nu}+u^{\mu}u_{\nu},$$

the projection onto the subspace of tangent space normal to u. The decomposition of the Weyl tensor yields its electric and magnetic contributions:

$$E_{\mu\nu}=C_{\mu\lambda\nu\sigma}u^{\lambda}u^{\sigma}, \quad \text{(A4)}$$

$$B_{\mu\nu}=\frac{1}{2}C_{\mu\lambda\gamma\delta}u^{\lambda}\eta^{\gamma\delta}_{\nu\sigma}u^{\sigma}, \quad \text{(A5)}$$

where $\eta^{\alpha\beta\gamma\delta}$ denotes the totally antisymmetric four-tensor with $\eta_{0123}=\sqrt{-g}$. Due to symmetry properties and the tracelessness of the Weyl curvature, E and B are symmetric and traceless, and they fully determine the Weyl curvature. One easily checks that $E_{\mu\nu}$ and $B_{\mu\nu}$ are also conformally invariant. We now want to perform the corresponding decomposition for the energy-momentum tensor of the scalar field ϕ:

$$T^{S}_{\mu\nu}=\phi,_{\mu}\phi,_{\nu}-\frac{1}{2}g_{\mu\nu}\phi^{,\lambda}\phi,_{\lambda}.$$

We define

$$\rho_S\equiv T^{(S)}_{\mu\nu}u^{\mu}u^{\nu}, \quad \text{(A6)}$$

$$p_S\equiv\frac{1}{3}T^{(S)}_{\mu\nu}h^{\mu\nu}, \quad \text{(A7)}$$

$$q_{\mu}\equiv-h^{\nu}_{\mu}T^{(S)}_{\nu\alpha}u^{\alpha}, \quad q_i=-\frac{1}{a}T^{(S)}_{0i}, \quad \text{(A8)}$$

$$\tau_{\mu\nu}\equiv h^{\alpha}{}_{\mu}h^{\beta}{}_{\nu}T^{(S)}_{\alpha\beta}-h_{\mu\nu}p_S. \quad \text{(A9)}$$

We then can write

$$T^{(S)}_{\mu\nu}=\rho_S u_{\mu}u_{\nu}+p_S h_{\mu\nu}+q_{\mu}u_{\nu}+u_{\mu}q_{\nu}+\tau_{\mu\nu}. \quad \text{(A10)}$$

This is the most general decomposition of a symmetric second-rank tensor. It is usually interpreted as the energy-momentum tensor of an imperfect fluid. In the frame of an observer moving with four-velocity u, ρ_S is the energy density of the scalar field, p_S is the isotropic pressure, q is the energy flux, $u\cdot q=0$, and τ is the tensor of anisotropic stresses, $\tau_{\mu\nu}h^{\mu\nu}=\tau_{\mu\nu}u^{\mu}=0$.

We now want to focus on a perturbed Friedmann universe. We therefore consider a four-velocity field u which deviates only in first order from the Hubble flow: $u=(1/a)\partial_0+\text{first order}$. Friedmann universes are conformally flat, and we require the scalar field to be a small perturbation on a Universe dominated by radiation and cold dark matter (CDM). The energy-momentum tensor of the scalar field and the Weyl tensor are thus of first order, and (up to first order) their decomposition does not depend on the choice of the first-order contribution to u, they are gauge invariant. But the decomposition of the dark matter depends on this choice. Cold dark matter is a pressureless perfect fluid. We can thus choose u to denote the energy flux of the dark matter, $T^{\mu}_{\nu}u^{\nu}=-\rho_C u^{\mu}$. Then the energy-momentum tensor of the dark matter has the simple decomposition

$$T^{(C)}_{\mu\nu}=\rho_C u_{\mu}u_{\nu}. \quad \text{(A11)}$$

With this choice, the Einstein equations (A3) linearized about an $\Omega=1$ Friedmann background with $T^{(S)}_{\rm background}=0$ yield the following ''Maxwell equations'' for E and B [42].

(i) Constraint equations:

$$\partial^i B_{ij}=4\pi G\,\eta_{j\beta\mu\nu}u^\beta q^{[\mu;\nu]}, \tag{A12}$$

$$\partial^i E_{ij}=8\pi G\left(\frac{1}{3}a^2\rho_C D_{,j}+\frac{1}{3}a^2\rho_S{}_{,j}-\frac{1}{2}\partial^i\tau_{ij}-\frac{\dot a}{a^2}q_j\right). \tag{A13}$$

(ii) Evolution equations:

$$a\dot B_{ij}+\dot a B_{ij}-a^2 h^\alpha_{(i}\eta_{j)\beta\gamma\delta}u^\beta E^{\gamma;\delta}_\alpha = -4\pi G a^2 h_{\alpha(i}\eta_{j)\beta\mu\nu}u^\beta\tau^{\alpha\mu;\nu} \tag{A14}$$

$$\dot E_{ij}+\frac{\dot a}{a}E_{ij}+a h^\alpha_{(i}\eta_{j)\beta\gamma\delta}u^\beta B^{\gamma;\delta}_\alpha = -4\pi G\left(aq_{ij}-\frac{\dot a}{a}\tau_{ij}+\dot\tau_{ij}+a\rho_C u_{ij}\right), \tag{A15}$$

where $(i,\ldots,j)$ denotes symmetrization in the indices i and j. The symmetric traceless tensor fields $q_{\mu\nu}$ and $u_{\mu\nu}$ are defined by

$$q_{\mu\nu}=q_{(\mu;\nu)}-\frac{1}{3}h_{\mu\nu}q^\lambda_{;\lambda},$$

$$u_{\mu\nu}=u_{(\mu;\nu)}-\frac{1}{3}h_{\mu\nu}u^\lambda_{;\lambda}.$$

In Eqs. (A14) and (A15), we have also used that, for the dark matter perturbations, only scalar perturbations are relevant, vector perturbations decay quickly. Therefore, u is a gradient field, $u_i=U_{;i}$ for some suitably chosen function U. Hence, the vorticity of the vector field u vanishes, $u_{[\mu;\nu]}=0$. With

$$\eta_{0ijk}=a^4\epsilon_{ijk},\quad \rho_S=a^{-2}T^S_{00},\quad q_i=-a^{-1}T^S_{0i},$$

we obtain, from Eq. (A13),

$$\partial^i E_{ij}=8\pi G\left(\frac{1}{3}\rho_C a^2 D_{,j}+\frac{1}{3}T^S_{00,j}-\frac{1}{2}\partial_i\tau_{ij}+\frac{\dot a}{a}T^S_{0j}\right). \tag{A16}$$

In Eq. (A16) and the following equations, summation over double indices is understood, irrespective of their position.

To obtain the equation of motion for the magnetic part of the Weyl curvature, we take the time derivative of Eq. (A14), using $u=(1/a)\partial_0+1.\text{order}$ and $\eta_{0ijk}=a^4\epsilon_{ijk}$. This leads to

$$(aB_{ij})^{\cdot\cdot}=-a\left\{\epsilon_{lm(i}\left[\dot E_{j)l}+\frac{\dot a}{a}E_{j)l}\right]_{,m}-4\pi G\,\epsilon_{lm(i}\left[\dot\tau_{j)l,m}+\frac{\dot a}{a}\tau_{j)l,m}\right]\right\}, \tag{A17}$$

where we have again used u as a gradient field and thus terms such as $\epsilon_{ijk}u_{lj,k}$ vanish. We now insert Eq. (A15) into the first square bracket above and replace product expressions of the form $\epsilon_{ijk}\epsilon_{ilm}$ and $\epsilon_{ijk}\epsilon_{lmn}$ with double- and triple-Kronecker deltas. Finally, we replace divergences of B with the help of Eq. (A12). After some algebra, one obtains

$$\epsilon_{lm(i}\left[\dot E_{j)l}+\frac{\dot a}{a}E_{j)l}\right]_{,m}=-\nabla^2 B_{ij}-4\pi G\,\epsilon_{lm(i}\left[2aq_{l,mj)}+\dot\tau_{jl,m}-\frac{\dot a}{a^2}\tau_{jl,m}\right].$$

Inserting this into Eq. (A17) and using $aq_l=-T^S_{0l}=-\dot\phi\phi_{,i}$, we finally find the equation of motion for B:

$$a^{-1}(aB)^{\cdot\cdot}_{ij}-\nabla^2 B_{ij}=8\pi G\mathscr{S}^{(B)}_{ij}, \tag{A18}$$

with

$$\mathscr{S}^{(B)}_{ij}=\epsilon_{lm(i}[-T^S_{0l,j)m}+\dot\tau_{j)l,m}],$$

and

$$\tau_{ij}=\phi_{,i}\phi_{,j}-\frac{1}{3}\delta_{ij}(\nabla\phi)^2. \tag{A19}$$

Since dark matter only induces scalar perturbations and B_{ij} consists of vector and tensor perturbations, it is independent of the dark matter fluctuations. Equations (A16) and (A18) are used in Sec. II, where we need $\partial^i E_{ij}$ and B_{ij} as source terms in the Liouville equation.

[1] G.F. Smoot *et al.*, Astrophys. J. **396**, L1 (1992); E.L. Wright *et al., ibid.* **396**, L13 (1992).

[2] D. Scott, J. Silk, and M. White, Science **268**, 829 (1995); E.J. Wollack, N.C. Jarosik, C.B. Netterfield, L.A. Page, and D. Wilkinson, Astrophys. J. Lett. **419**, L49 (1993); P. Meinhold *et al., ibid.* **409**, L1 (1993); T. Gaier, J. Schuster, J. Gundersen, T. Koch, M. Seiffert, P. Meinhold, and P. Lubin, Astrophys. J. **398**, L1 (1992); M.J. Devlin *et al.*, Astrophys. J. Lett. **430**, L1 (1994); E.L. Wright, G.F. Smoot, C.L. Bennett, and P.M. Lubin, Astrophys. J. **436**, 443 (1994), and references therein.

[3] P.J.E. Peebles and J. Silk, Nature (London) **436**, 233 (1990).

[4] N. Sugiyama and N. Gouda, Prog. Theor. Phys. **88**, 803 (1992).

[5] J.A. Peacock and S.J. Dodds, Mon. Not. R. Astron. Soc. **258**, P1 (1992).

[6] W. Hu, E.F. Bunn, and N. Sugiyama, Report No. CfPA-TH-94-01, astro-ph/9501034, 1995 (unpublished).

[7] J.P. Ostriker, Annu. Rev. Astron. Astrophys. **31**, 689 (1993).

[8] J. Holtzman, Astrophys. J. Suppl. Ser. **71**, 1 (1989).

[9] S. Xiang and T. Kiang, Mon. Not. R. Astron. Soc. **259**, 761 (1992).

[10] M. Davis, F.J. Summers, and D. Schlegel, Nature (London) **359**, 393 (1992); A.N. Taylor and M. Rowan-Robinson, *ibid.* **359**, 396 (1992).

[11] N. Bahcall, in *Seventeenth Texas Symposium on Relativistic Astrophysics and Cosmology*, Munich, Germany, 1994, edited

by H. Böhringer, G.E. Morfill, and J. Trümper (New York Academy of Sciences, New York, 1995).
[12] T.W.B. Kibble, J. Phys. A **9**, 1387 (1976).
[13] I. Chuang, R. Durrer, N. Turok, and B. Yurke, Science **251**, 1336 (1991).
[14] K.M. Gorski *et al.*, Astrophys. J. **430**, L85 (1994); K.M. Gorski, *ibid.* **430**, L89 (1994).
[15] N. Turok, Phys. Rev. Lett. **63**, 2625 (1989).
[16] R. Durrer, in *Formation and Interactions of Topological Defects*, edited by A.C. Davis and R. Brandenberger (NATO ASI Series B: Physics, Vol. 349, New York Academy of Sciences, New York, 1995), p. 255.
[17] D. Bennett and S.H. Rhie, Astrophys. J. **406**, L7 (1993).
[18] U.-L. Pen, D.N. Spergel, and N. Turok, Phys. Rev. D **49**, 692 (1994).
[19] R. Durrer, A. Howard, and Z.H. Zhou, Phys. Rev. D **49**, 681 (1994).
[20] D. Coulson, P. Ferreira, P. Graham, and N. Turok, Nature (London) **368**, 27 (1994).
[21] R. Durrer and Z.-H. Zhou, Phys. Rev. Lett. **74**, 1701 (1995).
[22] J.M. Stewart, *Non-Equilibrium Relativistic Kinetic Theory*, Springer Lecture Notes in Physics, Vol. 10, edited by J. Ehlers, K. Hepp, and H.A. Wiedenmüller (Springer-Verlag, Berlin, 1971).
[23] Y. Choquet-Bruhat, C. DeWitt-Morette, and M. Dillard-Bleick, *Analysis, Manifolds and Physics* (North-Holland, Amsterdam, 1982).
[24] M. Bruni, P.K.S. Dunsby, and G.F.R. Ellis, Astrophys. J. **395**, 34 (1992).
[25] R. Durrer, Fundamentals Cosmic Phys. **15**, 209 (1994).
[26] J.C.R Magueijo, Phys. Rev. D **46**, 3360 (1992).
[27] H. Kodama and M. Sasaki, Prog. Theor. Phys. Suppl. **78**, 1 (1984).
[28] J.M. Stewart and M. Walker, Proc. R. Soc. London A **341**, 49 (1974).
[29] R. Durrer, Phys. Rev. D **42**, 2533 (1990).
[30] P. Mészáros, Astron. Astrophys. **37**, 225 (1974).
[31] T.W.B. Kibble, in Ref. [16].
[32] W. Press, D. Spergel, and B. Ryden, Astrophys. J. **347**, 590 (1989).
[33] W.H. Press, B.P. Flannery, S.A. Teukolsky, and W.T. Vetterling, *Numerical Recipes* (Cambridge University Press, Cambridge, England, 1990).
[34] J. Borrill, E.J. Copeland, A.R. Liddle, A. Stebbins, and S. Veeraraghavan, Phys. Rev. D **50**, 2469 (1994), and references therein.
[35] J. Borrill, Phys. Rev. D **50**, 3676 (1994).
[36] N. Turok and D.N. Spergel, Phys. Rev. Lett. **64**, 2736 (1990).
[37] E.J. Groth and P.J.E. Peebles, Astron. Astrophys. **41**, 143 (1975).
[38] G. Efstathiou, in *Physics of the Early Universe*, edited by J.A. Peacock, A.F. Heavens, and A.T. Davies (Scottish Universities Summer School, Edinburgh, 1990).
[39] K.B. Fisher, M. Davis, M.A. Strauss, A. Yahil, and J.P. Huchra, Astrophys. J. **402**, 42 (1993).
[40] M White and E.F. Bunn, Berkeley Report No. CfPA-95-TH-02, 1995 (unpublished).
[41] R. Cen and J. Ostriker, Astrophys. J. Lett. **399**, L113 (1992).
[42] G.F.R.S. Ellis, *Varenna Summer School on General Relativity and Cosmology* XLVII Corso (Academic, New York, 1971).
[43] R. Durrer, A. Gangui, and M. Sakellariadou, Phys. Rev. Lett. **76**, 579 (1996).